AIP | Applied Physics Letters

Magnetocaloric properties of La(Fe,Si)13-based material and its hydride prepared by industrial mischmetal

L. F. Bao, F. X. Hu, L. Chen, J. Wang, J. R. Sun et al.

Citation: Appl. Phys. Lett. **101**, 162406 (2012); doi: 10.1063/1.4760262

View online: http://dx.doi.org/10.1063/1.4760262

View Table of Contents: http://apl.aip.org/resource/1/APPLAB/v101/i16

Published by the American Institute of Physics.

Related Articles

Giant magnetocaloric effects near room temperature in Mn1−xCuxCoGe
Appl. Phys. Lett. 101, 242405 (2012)

Magnetic phase transitions and magnetocaloric effect in La0.7Ca0.3Mn1-xFexO3 0.00≤x≤0.07 manganites
J. Appl. Phys. 112, 113901 (2012)

Oscillating magnetocaloric effect on graphenes
Appl. Phys. Lett. 101, 222405 (2012)

Crystallography, magnetic, and magnetocaloric properties of Gd57.5Co20Al22.5 alloy
J. Appl. Phys. 112, 103916 (2012)

Enthalpy change in the magnetocaloric effect
J. Appl. Phys. 112, 103912 (2012)

Additional information on Appl. Phys. Lett.

Journal Homepage: http://apl.aip.org/

Journal Information: http://apl.aip.org/about/about_the_journal

Top downloads: http://apl.aip.org/features/most_downloaded

Information for Authors: http://apl.aip.org/authors

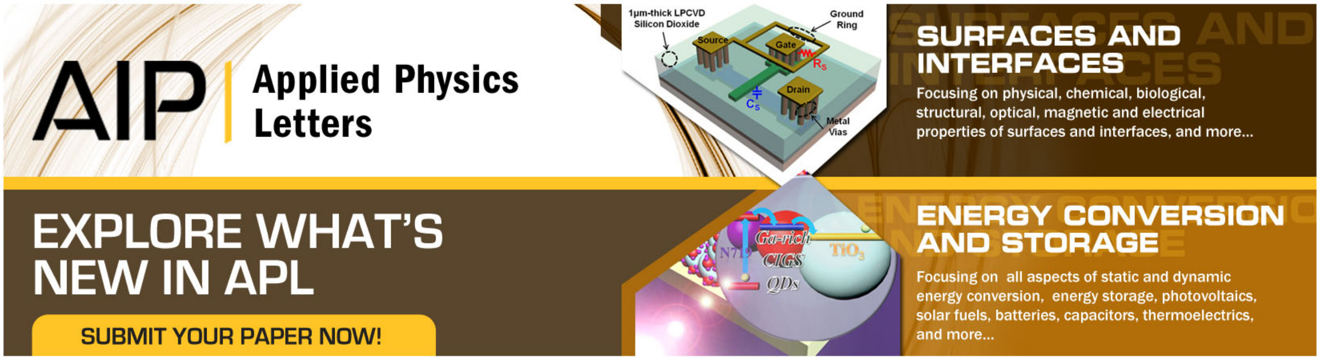

APPLIED PHYSICS LETTERS **101**, 162406 (2012)

Magnetocaloric properties of La(Fe,Si)$_{13}$-based material and its hydride prepared by industrial mischmetal

L. F. Bao, F. X. Hu,[a] L. Chen, J. Wang, J. R. Sun, and B. G. Shen
Beijing National Laboratory for Condensed Matter Physics and State Key Laboratory of Magnetism, Institute of Physics, Chinese Academy of Sciences, Beijing 100190, People's Republic of China

(Received 7 June 2012; accepted 3 October 2012; published online 18 October 2012)

Here, we choose La-Ce-Pr-Nd industrial mischmetal with low purity as raw material to prepare La(Fe,Si)$_{13}$-based magnetocaloric material and its hydride. It is demonstrated that the introduced impurities in the starting materials do not impair the formation of NaZn$_{13}$-type structure. The multi-replacement of La by magnetic atoms Ce,Pr,Nd enhances Curie temperature T_C while keeps the strong itinerant electron metamagnetic behavior. As a result, good magnetocaloric (MCE) properties appear in La$_{0.7}$(Ce,Pr,Nd)$_{0.3}$Fe$_{11.6}$Si$_{1.4}$ (LRFS) compound. The incorporation of interstitial H atom remarkably reduces hysteresis loss while increases T_C to 314 K. The effective refrigeration capacity after deducting hysteresis can be increased by ~128% upon H doping. © *2012 American Institute of Physics*. [http://dx.doi.org/10.1063/1.4760262]

The magnetocaloric effect (MCE) is characterized by appearance of the isothermal entropy change (ΔS) and adiabatic temperature change (ΔT_{ad}) due to a variable magnetic field, which is initially found in iron by Warburg.[1] This magneto-thermodynamic phenomenon provides the possibility of application of magnetic refrigeration technology which is more efficient and environmental than conventional gas compression technology. Over the years, several materials with large MCE have been discovered, such as Gd$_2$Si$_2$Ge$_2$,[2] MnFeP$_{0.45}$As$_{0.55}$,[3] MnAs$_{1-x}$Sb$_x$,[4] La(Fe,Si)$_{13}$-based compounds.[5,6] Among these materials, La(Fe,Si)$_{13}$-based compounds attracted much attention due to the tunable T_C, tunable transition nature, nontoxic character, low cost.[5–8] This material has been applied in demo-machine and high performance was confirmed.[9,10] The large MCE originates from field-induced itinerant electron metamagnetic (IEM) transition from paramagnetic (P) to ferromagnetic (F) state and concurrent lattice expansion. People made lots of effort to improve MCE. Rare-earth (R) elements, such as Ce, Pr, Nd, were individually introduced to substitute La and the effect on magnetocaloric properties was investigated.[11,12] It was found that lattice shrinks with the addition of Ce or Pr or Nd due to lanthanide contraction. The strong competition between magnetovolume effect and R-T (rare-earth and transition metal) coupling makes Curie temperature T_C shift in a very wide temperature range, meanwhile IEM behavior is strengthened and MCE enhances with increasing R elements. In most cases, the starting materials for preparing La(Fe,Si)$_{13}$-based magnetocaloric materials are individual elements. However, one knows that the four light rare earths of La, Ce, Pr, Nd account for 97% of the total R deposits on the earth, and most importantly, these four coexist in high ratio up to 92%–98% of total R in many nature minerals (for example, the ratio reaches to 98.6% in bastnasite located at California, USA). To purify the mixed La, Ce, Pr, Nd metal with nature ratio and industrial purity (the so-called LaCePrNd mischmetal) is much easier compared to get individual ones, and the cost is correspondingly lower. In this work, we choose La-Ce-Pr-Nd mischmetal with industrial purity as raw material to prepare La(Fe,Si)$_{13}$-based magnetocaloric material and its hydride. The influence of multi-replacement of La by magnetic atoms Ce, Pr, Nd on magnetic and magnetocaloric properties is firstly reported.

On the other hand, impurity effect is a crucial problem for the preparation of giant MCE materials. The discovery of giant MCE in Gd-Si-Ge in 1997 stimulated high interest. However, ultra-purified Gd was usually required to synthesize the giant MCE material.[13,14] It has been reported that the coexistence of impurities in commercial Gd weakens the first-order transition and reduces giant MCE. In this work, we also studied the effect of high impurities in La-Ce-Pr-Nd mischmetal on the phase formation of NaZn$_{13}$-type structure and MCE properties of the resulted compounds.

The commercial La-Ce-Nd-Pr mischmetal with industrial purity (99 wt. %) and natural ratio similar to that in minerals (La/Re ~ 28.27 wt. %, Ce/Re ~ 50.46 wt. %, Pr/Re ~ 5.55 wt. %, Nd/Re ~ 15.66 wt. %) was used to prepare La$_{0.7}$(Ce,Pr,Nd)$_{0.3}$Fe$_{11.6}$Si$_{1.4}$ alloys by conventional arc-melting technique. The purity and ratio was checked by inductively coupled plasma-atomic emission spectrometry (ICP-AES) and inductively coupled plasma mass spectrometry (ICP-MS), along with energy-dispersive x-ray spectroscopy (EDX). The lacked La in the formula was supplied by pure La with purity of 99.9 wt. %. La$_{0.7}$(Ce,Pr,Nd)$_{0.3}$Fe$_{11.6}$Si$_{1.4}$ is equal to La$_{0.7}$Ce$_{0.213}$Pr$_{0.023}$Nd$_{0.064}$Fe$_{11.6}$Si$_{1.4}$. Compared to La$_{0.7}$Ce$_{0.3}$Fe$_{11.6}$Si$_{1.4}$ (LCFS), near 30 at. % of Ce has been replaced by Pr and Nd. The resulted ingots were subsequently annealed at 1080 °C for 30 days and then quenched in liquid nitrogen. The hydrogen absorption was performed by further annealing the samples under hydrogen gas atmosphere in commercial P-C-T (pressure-composition-temperature) apparatus. The samples for hydrogenation are particles with diameter about 1 mm. The sample mass for magnetic measurement is around 3 mg. Powder x-ray diffraction using Cu Ka radiation was carried out to identify

---

[a] Author to whom correspondence should be addressed. Electronic addresses: fxhu@iphy.ac.cn and hufx@g203.iphy.ac.cn.

structure and coexistent impurity phases. Magnetic measurements were performed using a superconducting quantum interference device (MPMS SQUID VSM, Quantum Design^{TM}, USA).

Powder x-ray diffraction patterns confirmed that both $La_{0.7}(Ce,Pr,Nd)_{0.3}Fe_{11.6}Si_{1.4}$ alloy and its hydride $La_{0.7}(Ce,Pr,Nd)_{0.3}Fe_{11.6}Si_{1.4}H_{1.6}$ (LRFSH) crystallize in the cubic $NaZn_{13}$-type structure (1:13 phase) with space group $Fm\bar{3}c$. A little amount of impurity phases were detected, which were identified to be α-Fe and tetragonal Cu_2Sb-type LaFeSi (1:1:1 phase, space group P4/nmm). No other impurity phases were detected besides α-Fe and 1:1:1 structure. Rietveld refinements revealed that the ratio of 1:13, α-Fe, 1:1:1 phase is 93.2%, 1.7%, 5.1% and 94.0%, 1.4%, 4.6% for $La_{0.7}(Ce,Pr,Nd)_{0.3}Fe_{11.6}Si_{1.4}$ and the hydride, respectively (Fig. 1). One can notice that hydrogenation process does not make the ratio of impurity phases change much. For comparison, we also refine the structure for the similar composition $La_{0.7}Ce_{0.3}Fe_{11.6}Si_{1.4}$ prepared by individual La and Ce (La, Ce purity: 99.9%) under same conditions. The ratio of 1:13, α-Fe, and 1:1:1 phase is 97.2%, 0.47%, and 2.3%, respectively. One can notice the clear difference of 1:1:1 phase ratio for the materials prepared by different starting materials. The 1:1:1 impurity phase in $La_{0.7}(Ce,Pr,Nd)_{0.3}Fe_{11.6}Si_{1.4}$ based on mischmetal is about two times higher than that in $La_{0.7}Ce_{0.3}Fe_{11.6}Si_{1.4}$. Generally, as-cast $La(Fe,Si)_{13}$ ingots without annealing contain little 1:13 phase. The main phase is α-Fe, coexistent with 1:1:1 phase.[15,16] Upon post-annealing, 1:13 phase can be produced by peritectic reaction: L_{La} (LaFeSi 1:1:1 phase) + $\alpha\text{-Fe} \rightarrow La(Fe,Si)_{13}$.[15] The observation of higher 1:1:1 phase in $La_{0.7}(Ce,Pr,Nd)_{0.3}Fe_{11.6}Si_{1.4}$ and its hydride may indicate more incomplete peritectic reaction during post annealing. The high impurities in the starting material of mischmetal might lower the atom diffusivity and make the peritectic reaction incomplete.

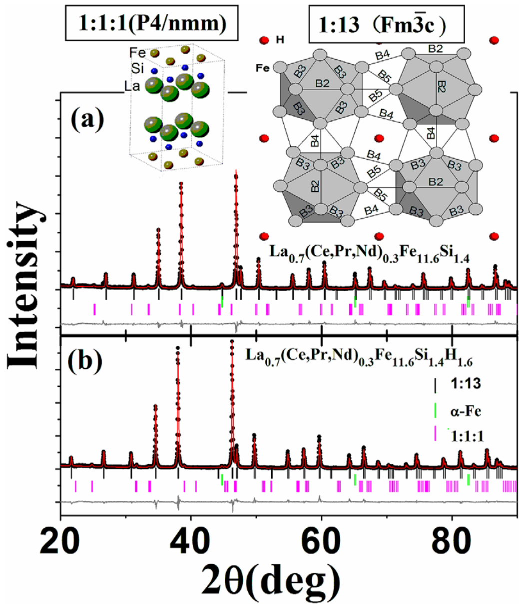

FIG. 1. Rietveld refinement plots for (a) $La_{0.7}(Ce,Pr,Nd)_{0.3}Fe_{11.6}Si_{1.4}$ and (b) the hydride $La_{0.7}(Ce,Pr,Nd)_{0.3}Fe_{11.6}Si_{1.4}H_{1.6}$. Black point and red line represent observed and calculated profiles, respectively, and the difference between them is shown at the bottom of each graph. The vertical bars represent the Bragg reflection positions of $NaZn_{13}$-type (top), α-Fe (middle), and LaFeSi (bottom). Insets of (a) schematically show the 1:1:1 and 1:13 structure. The locations of the Fe-Fe bonds in 1:13 phase are also indicated.

Report on LaFeSi tetragonal 1:1:1 structure is rather limited, particularly for the details upon H absorption. Fig. 2 displays the separated XRD patterns of 1:1:1 structure from Fig. 1 for $La_{0.7}(Ce,Pr,Nd)_{0.3}Fe_{11.6}Si_{1.4}$ and its hydride, compared to that in $La_{0.7}Ce_{0.3}Fe_{11.6}Si_{1.4}$. One can notice that c axis of $La_{0.7}(Ce,Pr,Nd)_{0.3}Fe_{11.6}Si_{1.4}$ contracts with addition of small R atoms, Pr and Nd, while a axis keeps nearly unchanged compared to $La_{0.7}Ce_{0.3}Fe_{11.6}Si_{1.4}$ (see Table I). However, H absorption notably elongates the 1:1:1 lattice: c axis is elongated in expense of a axis contract. Correspondingly, XRD pattern changes much. One can notice the clear differences of peak positions of 1:1:1 structure between $La_{0.7}(Ce,Pr,Nd)_{0.3}Fe_{11.6}Si_{1.4}$ and its hydride (Fig. 2). This might be one reason why the 1:1:1 impurity phases in 1:13 alloys were sometimes improperly identified to be other phases. Furthermore, we notice that 1:1:1 lattice also notably expands upon hydrogenation (Table I). The lattice volume expands by 3.5% and 7.9% ($(V_H\text{-}V)/V$) for 1:13 and 1:1:1 structure, respectively, indicating H atoms surely enter the 1:1:1 lattice similar to the case in 1:13 structure. However, the occupation of H atoms in 1:1:1 structure is not clear at the moment though one knows that the interstitial H/C atoms occupy 24d site in 1:13 structure.[17]

In Table I, we summarized the refined results, phase ratio, lattice parameter/volume, Fe-Fe bond length (B1, B2, B3, B4, B5) in 1:13 structure for $La_{0.7}Ce_{0.3}Fe_{11.6}Si_{1.4}$, $La_{0.7}(Ce,Pr,Nd)_{0.3}Fe_{11.6}Si_{1.4}$ and its hydride. During refinements, we suppose the introduced Ce, Pr, and Nd randomly occupy La sites in 1:13 structure. One can notice that B4 bond in $La_{0.7}(Ce,Pr,Nd)_{0.3}Fe_{11.6}Si_{1.4}$ is still the shortest one among the five (B4 location can be found in the inset of Fig. 1). The multisubstitution of Ce, Pr, Nd for La makes the 1:13 lattice shrink due to the smaller atomic radius of Pr/Nd than Ce. B1, B3, and B4 bond become shorter while B2 and B5 become longer, compared to that in $La_{0.7}Ce_{0.3}Fe_{11.6}Si_{1.4}$. Upon hydrogenation lattice expands as expected, and all Fe-Fe bonds are getting longer and the shortest B4 changes the most (see the inset of Fig. 1(b)). This fact can be easily understandable noting that the 24d interstitial site, occupied by H, is surrounded

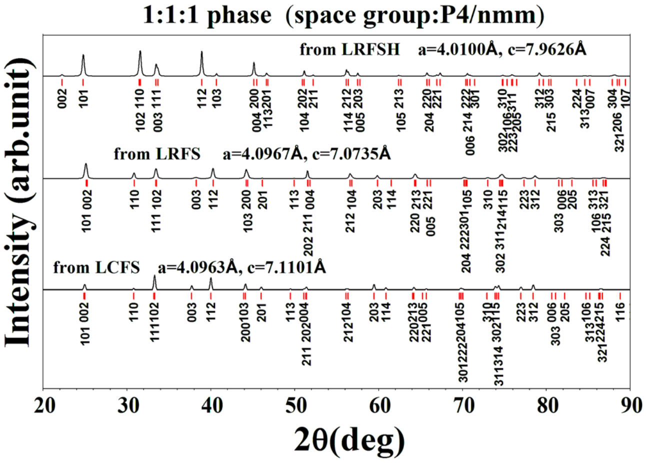

FIG. 2. The separated XRD patterns of 1:1:1 structure from Fig. 1 for LRFS and the hydride LRFSH, compared to that in LCFS.

TABLE I. Refined results including phase ratio, lattice parameter/volume, Fe-Fe bond length (B1, B2, B3, B4, B5) in 1:13 structure, and Curie temperature T_C, entropy change $-\Delta S$, effective refrigeration capacity RC_{effe} for LCFS, LRFS, and the hydride LRFSH.

	LCFS	LRFS	LRFSH
1:13 (wt. %)	97.2	93.2	94.1
α-Fe (wt. %)	0.5	1.7	1.3
1:1:1 (wt. %)	2.3	5.1	4.6
$a_{1:13}$ (Å)	11.4576(5)	11.4525(3)	11.5861(6)
$a_{1:1:1}$ (Å)	4.0963(3)	4.0966(5)	4.0099(5)
$c_{1:1:1}$ (Å)	7.1101(2)	7.0735(0)	7.9626(0)
B1 (Å)	2.4610(6)	2.4553(4)	2.4732(1)
B2 (Å)	2.6696(3)	2.6853(7)	2.6878(5)
B3 (Å)	2.5678(4)	2.5567(7)	2.5793(4)
B4 (Å)	2.4390(7)	2.4346(3)	2.4833(7)
B5 (Å)	2.4704(2)	2.4926(7)	2.5107(9)
$V_{1:13}$ (Å^3)	1504.14	1502.12	1555.32
$V_{1:1:1}$ (Å^3)	119.31	118.71	128.04
R_{wp} (%)	11.8	9.4	9.7
T_c (K)	163	169	314
$-\Delta S$ (J/kgK)	28.2	29.1	25.4
RC_{eff} (J/kg)	136	166	379

by B4 bond (see the right inset in Fig. 1). All the changes in structure predict changes in magnetic properties.

Fig. 3 displays temperature-dependent magnetization measured under 0.02 T for $La_{0.7}(Ce,Pr,Nd)_{0.3}Fe_{11.6}Si_{1.4}$ and its hydride, compared to that of $La_{0.7}Ce_{0.3}Fe_{11.6}Si_{1.4}$. One can find Curie temperature, T_C, (∼169 K) of $La_{0.7}(Ce,Pr,Nd)_{0.3}Fe_{11.6}Si_{1.4}$ locates at a slightly higher temperature than that of $La_{0.7}Ce_{0.3}Fe_{11.6}Si_{1.4}$ (T_C ∼163 K, defined as the temperature at which the largest slope occurs on heating). The introduced stronger Pr-Fe, Nd-Fe than Ce-Fe ferromagnetic (FM) coupling in the mischmetal alloy should be responsible for the higher T_C.[11] Usually, the R-Fe (R = Ce, Pr, Nd) FM coupling enhances along the sequence of Ce, Pr, Nd. In a $La(Fe,Si)_{13}$-based compound, magnetic moment completely comes from Fe noting La is a non-magnetic atom. However, the Fe-Fe interactions critically depend on bond length. As the bond length is shorter than 2.45 Å, anti-ferromagnetic coupling prevails in rich-Fe compounds, but ferromagnetic coupling shows up and becomes stronger with elongating the bond length as Fe-Fe bond length is close but larger than 2.45 Å.[18] Previous studies indicated that replacement of La by individual Ce or Pr or Nd makes lattice shrink and T_C decrease. The decrease slope for Ce-doped $La_{1-x}Ce_xFe_{11.5}Si_{1.5}$ is consistent with that of $La(Fe,Si)_{13}$,[11] indicating the Fe-Fe coupling dominates the T_C, while the contribution from Ce-Fe coupling is negligibly weak. For the Pr/Nd-doped case, the lattice further contracts and T_C should further reduce if only Fe-Fe coupling was considered. However, the T_C appears at a higher temperature than Ce-doped case due to the stronger Pr-Fe, Nd-Fe coupling.[11] Thus, it is easily understandable that the multi-replacement of La by Ce, Pr, Nd will enhance T_C compared to the case of single-replacement of La by Ce.

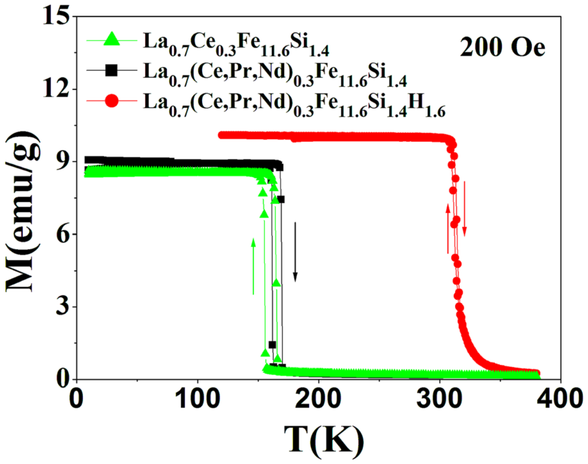

FIG. 3. Temperature-dependent magnetization measured under 0.02 T for $La_{0.7}(Ce,Pr,Nd)_{0.3}Fe_{11.6}Si_{1.4}$ and the hydride $La_{0.7}(Ce,Pr,Nd)_{0.3}Fe_{11.6}Si_{1.4}H_{1.6}$, compared to that of $La_{0.7}Ce_{0.3}Fe_{11.6}Si_{1.4}$. Arrows indicate cooling/heating path.

H absorption enlarges the lattice and enhances the Fe-Fe FM coupling remarkably, thus T_C appears at a much higher temperature, ∼314 K, for $La_{0.7}(Ce,Pr,Nd)_{0.3}Fe_{11.6}Si_{1.4}H_{1.6}$. Along with the shift of T_C, first-order nature weakens. One can notice that the thermal hysteresis around transition is about 9 K and 8 K for $La_{0.7}Ce_{0.3}Fe_{11.6}Si_{1.4}$ and $La_{0.7}(Ce,Pr,Nd)_{0.3}Fe_{11.6}Si_{1.4}$, respectively, but nearly approaches to zero in the hydride $La_{0.7}(Ce,Pr,Nd)_{0.3}Fe_{11.6}Si_{1.4}H_{1.6}$. Figs. 4(a) and 4(b) show the representative magnetization isotherms of $La_{0.7}(Ce,Pr,Nd)_{0.3}Fe_{11.6}Si_{1.4}$ and its hydride on field increase and decrease. The maximal hysteresis loss (enclosed area in a field cycle) is 232 J/kg (Fig. 4(a)) for $La_{0.7}(Ce,Pr,Nd)_{0.3}Fe_{11.6}Si_{1.4}$, which is similar to that (241 J/kg) of $La_{0.7}Ce_{0.3}Fe_{11.6}Si_{1.4}$ (not shown), indicating the first-order nature and metamagnetic behavior remains strong upon the introduction of Pr and Nd. H absorption reduces the hysteresis remarkably. The maximal hysteresis loss is only 42 J/kg (Fig. 4(b)), which is reduced by 82% compared to its mother compound.

One knows that hydrogenating process enlarges the lattice and makes the sample loose or even pulverized. This fact prompts us to think that hydrogenation could also change the distribution of grain boundaries and reduce the internal strain, thus cause a reduction of hysteresis.[19] It has been proved[19,20] that the reduction of internal strain definitely reduces the hysteresis loss. As the sample is broken from bulk into fragments or particles, hysteresis loss becomes smaller due to the reduction of internal strain and the increase of surface area. The reduced ratio of hysteresis can be as high as ∼61% as the bulk is ground into particles with size 20–50 μm.[20] Various intrinsic and extrinsic factors can affect the hysteresis size. Intrinsic ones generally include band structure, impurity and nucleation factors, strain effect, frictions from domain rearrangements, while extrinsic ones refer to the thermal equilibrium and the situation of heat transfer during measurements, which closely relates to field/temperature sweep rate.[21] In our measurements, same field/temperature sweep rate and similar sample size were adopted for all samples, thus extrinsic reasons from thermal equilibrium/heat transfer should be excluded for the observed differences of hysteresis in different samples. Upon hydrogenation, the change of distribution of grain boundaries and the reduction of internal strain, along with the possible change of band structure[22] should

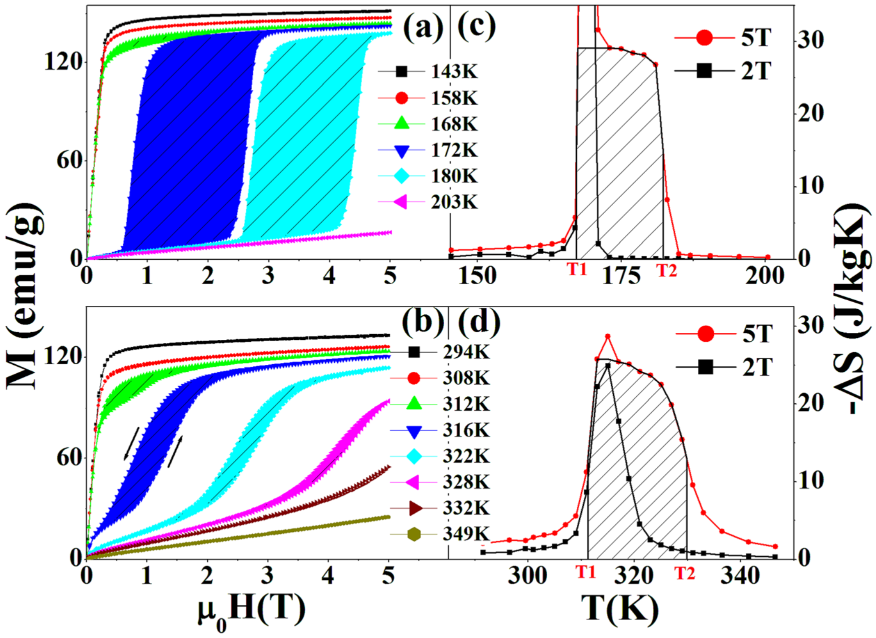

FIG. 4. Representative magnetization isotherms on field increase and decrease for (a) $La_{0.7}(Ce,Pr,Nd)_{0.3}Fe_{11.6}Si_{1.4}$ and (b) the hydride $La_{0.7}(Ce,Pr,Nd)_{0.3}Fe_{11.6}Si_{1.4}H_{1.6}$, where the shadow area indicates the hysteresis loss in a field cycle. Magnetic entropy change ΔS as a function of temperature under different fields for the corresponding samples was shown in (c) and (d).

be responsible for the remarkable reduction of hysteresis in the hydrides.

Notable reduction of hysteresis will enhance effective refrigeration capacity (RC_{effe}). We calculated magnetic entropy change ΔS from magnetization data collected on field increasing by using Maxwell relation $\Delta S(T,H) = \mu_0\int_0^H \left(\frac{\partial M}{\partial T}\right)_H dH$ (see Figs. 4(c) and 4(d)). The obtained effective ΔS_{effe} (not the spike but the high plateau value[23,24]) is −29.1 J/kgK (173 K), −25.4 J/kgK (317 K) under a field change of 0–5 T, for $La_{0.7}(Ce,Pr,Nd)_{0.3}Fe_{11.6}Si_{1.4}$ and its hydride, respectively. The direct refrigerant capacity (RC) evaluated by integrating the area (the shadow area in Figs. 4(c) and 4(d)) under ΔS curve from T_1 to T_2 (T_2-T_1: half-maximum width) is 398 J/kg, 421 J/kg, and the effective RC_{effe} after deducting the maximal hysteresis loss[25] is 166 J/kg, 379 J/kg for $La_{0.7}(Ce,Pr,Nd)_{0.3}Fe_{11.6}Si_{1.4}$ and its hydride, respectively. One can notice the effective RC_{effe} of the hydride enhances by ∼128% compared to its mother compound due to the remarkable reduction of hysteresis loss. The RC_{effe} value (∼379 J/kg, 314 K) of the present hydride $La_{0.7}(Ce,Pr,Nd)_{0.3}Fe_{11.6}Si_{1.4}H_{1.6}$ is larger than the RC_{effe} (evaluated by same method) of many other refrigerants at similar temperature range, such as $Gd_5Ge_{1.9}Si_2Fe_{0.1}$ (RC_{effe} ∼ 355 J/kg, 305 K),[25] $LaFe_{11.2}Co_{0.7}Si_{1.1}C_{0.1}$ (RC_{effe} ∼ 320 J/kg, 290 K),[7] and $La_{0.5}Pr_{0.5}Fe_{11.4}Si_{1.6}H_x$ (RC_{effe} ∼ 351 J/kg, 317 K).[26] For hydride $La_{0.7}Ce_{0.3}Fe_{11.6}Si_{1.4}H_{1.7}$, T_C locates at 316 K, 2 K different from that of $La_{0.7}(Ce,Pr,Nd)_{0.3}Fe_{11.6}Si_{1.4}H_{1.6}$ (T_C ∼ 314 K). Under 5 T, the effective ΔS_{effe} and RC_{effe} are 25.8J/kgK and 352 J/kg, respectively. The ΔS_{eff} is nearly the same, while RC_{effe} is slightly smaller compared to that of $La_{0.7}(Ce,Pr,Nd)_{0.3}Fe_{11.6}Si_{1.4}H_{1.6}$. All the results demonstrated that the $La(Fe,Si)_{13}$-based MCE materials prepared by industrial mischmetal can be an excellent choice for refrigerants.

In summary, we adopted La-Ce-Pr-Nd industrial mischmetal with low purity and nature ratio similar to that of minerals to prepare $La_{0.7}(Ce,Pr,Nd)_{0.3}Fe_{11.6}Si_{1.4}$ and its hydride. The structure, impurity effect, and MCE properties were studied. Our studies demonstrated that the impurities in the starting materials do not impair the formation of $NaZn_{13}$-type structure. The resulted $La_{0.7}(Ce,Pr,Nd)_{0.3}Fe_{11.6}Si_{1.4}$ and the hydride exhibit excellent MCE properties. The effective ΔS is −29.1 (173 K) and −25.4 J/kgK (317 K) under 5 T for the former and latter, respectively. The effective RC_{effe} upon hydrogenation enhances by 128% due to the notable reduction of hysteresis loss, while T_C shifts to 314 K. The good MCE properties, high RC_{effe}, and low cost of starting materials make the $La(Fe,Si)_{13}$-based materials prepared by industrial mischmetal highly attractive in view of promoting industrial production and practical applications.

This work was supported by the National Natural Science Foundation of China, the National Basic Research of China, the Hi-Tech Research and Development program of China, and the Knowledge Innovation Project of the Chinese Academy of Sciences.

[1] E. Warburg, Ann. Phys. Chem. (Leipzig) **13**, 141 (1881).
[2] V. K. Pecharsky and K. A. Gscheider, Jr., Phys. Rev. Lett. **78**, 4494 (1997).
[3] O. Tegus, E. Bruck, K. H. J. Buschow, and F. R. de Boer, Nature **415**, 150 (2002).
[4] H. Wade and Y. Tanabe, Appl. Phys. Lett. **79**, 3302 (2001).
[5] F. X. Hu, B. G. Shen, J. R. Sun, Z. H. Cheng, G. H. Rao, and X. X. Zhang, Appl. Phys. Lett. **78**, 3675 (2001).
[6] A. Fujita, S. Fujieda, Y. Hasegawa, and K. Fukamichi, Phys. Rev. B **67**, 104416 (2003).
[7] M. Balli, D. Fruchart, and D. Gignoux, Appl. Phys. Lett. **92**, 232505 (2008).
[8] B. G. Shen, J. R. Sun, F. X. Hu, H. W. Zhang, and Z. H. Cheng, Adv. Mater. **21**, 4545 (2009).
[9] S. Russek, J. Auringer, A. Boeder, J. Chell, S. Jacobs, and C. Zimm, in Fourth IIF-IIR International Conference on Magnetic Refrigeration at Room Temperature, Baotou, China, 23–28 August 2010.
[10] A. Fujita, S. Koiwai, S. Fujieda, K. Fukamichi, T. Kobayashi, H. Tsuji, S. Kaji, and A. Takahashi Saito, Jpn. J. Appl. Phys., Part 2 **46**, L154 (2007).
[11] L. Jia, J. R. Sun, J. Shen, Q. Y. Dong, F. X. Hu, T. Y. Zhao, and B. G. Shen. Appl. Phys. Lett. **92**, 182503 (2008).
[12] A. Fujita, S. Fujieda, and K. Fukamichi, J. Appl. Phys. **99**, 08K910 (2006).
[13] V. K. Pecharsky and A. Gschneidner, Jr., J. Magn. Magn. Mater. **167**, 179 (1997).
[14] V. K. Pecharsky and A. Gschneidner, Jr., J. Appl. Phys. **85**, 5365 (1999).
[15] V. Raghavan, J. Phase Equilib. **22**, 158 (2001).
[16] X. Chen, Y. G. Chen, and Y. B. Tang, J. Alloys Compd. **509**, 8534 (2011).

[17] O. Moze, W. Kockelmann, J. P. Liu, F. R. De Boer, and K. H. J. Buschow, J. Magn. Magn. Mater. **195**, 391 (1999).
[18] Z. W. Li and A. H. Morrish, Phys. Rev. B. **55**, 3670 (1997).
[19] J. D. Moore, G. K. Perkins, Y. Bugoslavsky, M. K. Chattopadhyay, S. B. Roy, P. Chaddah, V. K. Pecharsky, K. A. Gschneidner, Jr., and L. F. Cohen, Appl. Phys. Lett. **88**, 072501 (2006).
[20] F. X. Hu, L. Chen, J. Wang, L. F. Bao, J. R. Sun, and B. G. Shen, Appl. Phys. Lett. **100**, 072403 (2012).
[21] J. D. Moore, K. Morrison, K. G. Sandeman, M. Katter, and L. F. Cohen, Appl. Phys. Lett. **95**, 252504 (2009).
[22] J. Leib, J. E. Snyder, T. A. Lograsso, D. Schlagel, and D. C. Jiles, J. Appl. Phys. **95**, 6915 (2004).
[23] G. J. Liu, J. R. Sun, J. Shen, B. Gao, H. W. Zhang, F. X. Hu, and B. G. Shen, Appl. Phys. Lett. **90**, 032507 (2007).
[24] M. Balli, D. Fruchart, D. Gignoux, and R. Zach, Appl. Phys. Lett. **95**, 072509 (2009).
[25] V. Provenzano, A. J. Shapiro, and R. D. Shull, Nature (London) **429**, 853 (2004).
[26] J. L. Zhao, J. Shen, F. X. Hu, Y. X. Li, J. R. Sun, and B. G. Shen, J. Appl. Phys. **107**, 113911 (2010).